10.1109/ULTSYM.2011.0171

Ultrasound Current Source Density Imaging Using a Clinical Intracardiac Catheter

Qian Li, Yexian Qin, Pier Ingram, and Russell Witte
Department of Radiology
University of Arizona
Tucson, AZ 85724 USA
rwitte@email.arizona.edu

Zhaohui Wang
Department of Medicine
University of Pittsburgh
Pittsburgh, PA 15260 USA

Abstract— **Radiofrequency catheter ablation for treatment of cardiac arrhythmia requires pre-surgical mapping of the heart's activation wave. However, modern cardiac mapping systems continue to suffer from significant limitations. We have proposed Ultrasound Current Source Density Imaging (UCSDI) as a new modality to map reentry currents in the heart. In this study, we focus on interfacing UCSDI with a clinical intra-cardiac catheter—a key step towards translating UCSDI to the clinic for guiding cardiac ablation therapy. Sensitivity of UCSDI combined with the catheter was tested in a tissue mimicking phantom and fresh excised porcine hear tissue. Effect of the recoding distance on the detection of UCSDI was also investigated. Sensitivity of UCSDI with catheter was 4.7 μV/mA (R^2 = 0.999) in cylindrical gel (0.9% NaCl), and 3.2 μV/mA (R^2 = 0.92) in porcine heart tissue. The AE signal was detectable more than 25 mm away from the source in cylindrical gel (0.9% NaCl).**

Keywords-cardiac arrhythmia; catheter ablation; acousto-electric effect; ECG, EKG, multi-electrode recording

I. BACKGROUND AND THEORY

Cardiac arrhythmia is a serious health concern affecting more than 4 million Americans. Each year 500,000 receive radiofrequency catheter ablation for treatment. Catheter ablation therapy is completely curative for some types of arrhythmia [1]. It currently plays a pivotal role in the clinic for interventional treatment of arrhythmia.

Despite broad success of catheter ablation, the procedure depends on a pre-surgical electrophysiology (EP) study to obtain the detailed mapping of the heart's electrical system. This involves placing an electrode catheter into the heart and navigating it through the area of interest to collect multiple electrocardiograms (ECG). The most established EP guidance technique is fluoroscopy. Advanced mapping technologies, like electro-anatomical mapping (EAM), have been developed in recent years to facilitate mapping the cardiac activation wave with reduced exposure to ionizing radiation compared to fluoroscopy [2, 3]. Despite the high technological achievements, there still are factors limiting its functionality. For example, commercial mapping systems, such as the CARTO™ EAM system, are not able to monitor the cardiac activation wave in real-time, requiring averages over many cardiac cycles and, consequently, not capable of detecting non-sustained arrhythmias (e.g., ventricular tachycardia) [4, 5].

We have formerly proposed Ultrasound Current Source Density Imaging (UCSDI) as a new modality that potentially facilitates and enhances mapping biopotentials in the heart [6, 7] and brain [8]. In this study, we focus on using UCSDI for cardiac imaging. UCSDI is based on Ohm's Law and the acoustoelectric (AE) effect, which can be described as

$$\frac{\Delta\rho}{\rho_0} = -K\Delta P, \qquad (1)$$

where $\Delta\rho$ is the resistivity change, ρ_0 the direct current resistivity, ΔP the ultrasonic pressure and K the interaction constant. Equation (1) indicates that a change in local pressure induces a modulation of resistivity with the conversion efficiency determined by K, which has been measured in rabbit heart tissue and reported in our previous work [9]. The AE effect was first reported in the 1940's [10] and later proposed for electrical impedance tomography with applications for breast imaging [11, 12].

For UCSDI, the AE effect exclusively modulates a material's resistivity at the focal spot of an ultrasound beam. When current is applied to the material, this induces a local current density change and is detected in the form of voltage—the AE signal. The amplitude of the AE signal is affected by several factors [13, 14, 15, 16]. The AE signal is recorded with one or more electrodes at known ultrasonic pressure. A 3-D ultrasound currents source density image (UCSDI) of the electrical current density distribution is generated when the ultrasound beam is scanned across the tissue volume. In our recent work, 4-D UCSDI (space and time) was demonstrated for a fast time-varying current dipole field [17]. Pulse echo (PE) ultrasound is simultaneously acquired and co-registered with UCSDI. This provides additional information about the physical structure of the tissue or object being examined.

To translate UCSDI to the patients, a key steppingstone is to interface UCSDI with a clinical ultrasound system. In this study, we demonstrate that an existing commercial intra-cardiac catheter is capable of UCSDI. The combined system was tested by characterizing an artificially generated current pattern in both tissue-mimicking phantom and excised porcine heart tissue. Sensitivity of the combined system and the effect of the recording distance on sensitivity were investigated.

II. METHODS

A. Materials

Gel phantoms were made of 1.5% Agarose™ and 0.9% NaCl in deionized water. Gels were cast into cylinders with 55 to 60 mm thickness and 45 to 50 mm diameter. Dimensions as above were chosen to model the approximate thickness of the human myocardium. The central axis of the cylinder was made hollow to allow passage through the gel with approximately 2 mm diameter.

Fresh porcine hearts were obtained according to protocols approved by the Institutional Animal Care and Use Committee (IACUC) at the University of Arizona. Tissue slabs were excised off the left ventricle of the heart and wrapped around to allow a pathway in the middle. The samples were then fixed in shape with surgical suture. Care was taken during the extraction of the samples such that their final shape had dimensions of 40 to 50 mm along the long side (along the pathway in the middle) and 30 to 40 mm in cross section.

Sample was placed in a customized imaging chamber printed with a 3D rapid prototyping machine (Objet Connex350, Full cure 720). For gel phantoms, a special-made holder was placed on the side to prevent slippage during imaging. For heart tissue, warm gel (1.5% Agarose™ in deionized water) was poured in to the chamber and let cool down to room temperature to form a layer between the tissue and the bottom of the chamber. This helped keep the tissue in place during imaging, and minimize acoustic impedance mismatches.

An intra-cardiac catheter (Biosense Webster, CristaCath™, 7F, 20 electrode) was advanced through the pathway in the sample. Physiological saline (0.9% NaCl) could be added to the pathway to ensure good electrical contact.

B. Instrumentation

As depicted in Fig. 1, one pair of platinum electrodes was used to directly pass current (Agilent 33220A function generator, 200Hz) through the sample. A 1-ohm resistor was placed in series with the current injecting electrodes to measure the voltage across it and thus obtain the current amplitude, which was captured on the channel 1 of a low frequency data acquisition board (National Instruments PXI-6289). The catheter recorded the signal and branched into two differential amplifiers. One amplifier (Preamble 1855, 1 MHz bandwidth) was connected after an analog high pass filter (200 kHz cut-off-frequency) to record the high frequency AE signal, which was further amplified (Lecroy DA 1855A) by 50 times and captured on channel 2 of a high frequency data acquisition board (National Instruments PXI-5105). Another differential amplifier (Lecroy DA 1855A) captured the bypassed low frequency voltage signal, which was recorded on the channel 2 of the low frequency data acquisition board. A 1MHz single-element focused transducer (Panametrics, f = 68 mm, D = 38 mm) was pulsed every 400 µsec before, during and after the current injection (3 cycles at 200 Hz). The PE signal received by the transducer was simultaneously recorded on channel 1 of the high frequency data acquisition board. The transducer was scanned along or across the sample to form UCSDI and PE images.

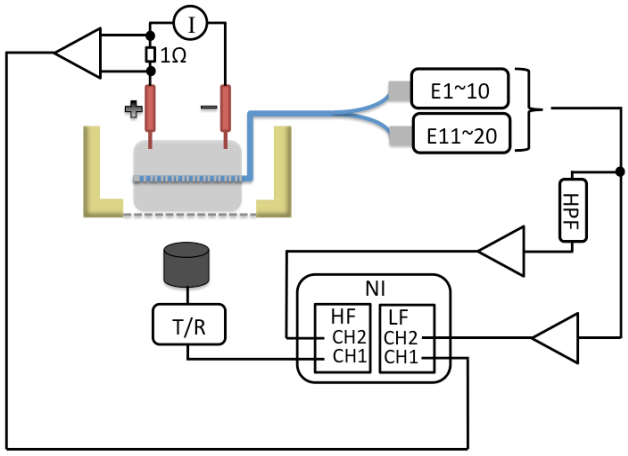

Figure 1. UCSDI System instrumentation. I represents the function generator. T/R is short for transmit/receive, which represents the ultrasound pulsar/receiver. NI denotes the National Instruments data acquisition system. HF and LF denote the high frequency and low frequency data acquisition boards respectively. CH 1 and 2 on the HF board are PE and AE channel respectively. CH 1 and 2 on the LF board are current and voltage channel respectively. E1~10 denotes the connecters for electrode 1~10 on the catheter. E11~20 denotes the connecters for electrode 11~20 on the catheter. HPF denotes high pass

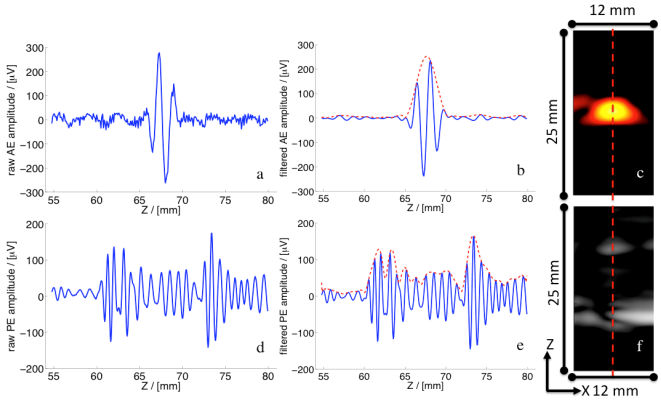

Figure 2. PE and UCSDI images of a current monopole in cylindrical gel and corresponding radiofrequency signals. Left column: unfiltered AE signal (a) and unfiltered PE signal (d). Middle column: bandpass filtered AE signal (b) and bandpass filtered PE signal (e). Red dashed lines delineate the envelopes of the radiofrequency signals. Right column: co-registered hot color UCSDI image (c) of a monopole.and gray scale PE image (f) Red dashed-line through the center of the images corresponds to the envelope of AE and PE signals in the middle column. Images are displayed in dB scale

III. RESULTS

A. Phantom study

Fig. 2 demonstrates the process of forming images from radiofrequency signals of a current monopole in a cylindrical gel. Raw radiofrequency AE signals (Fig. 2a) were acquired on the data acquisition system. The envelope (Fig. 2b, red dashed-line) was taken after band-pass filtering in the frequency domain to reduce noise. A series of AE signals were processed

the same way and formed into a UCSDI image of the monopole (Fig. 2c). Simultaneously acquired PE signals were processed in a similar fashion except that the space coordinates were calculated based on the two-way travel of ultrasound (Fig. 2d, 2e, 2f). Images presented in this paper were created following the same process.

AE signals from a monopole in a cylindrical gel were recorded with the same electrode on the catheter at different current levels (Fig. 3a). The magnitudes of the AE signals were used to generate a best-fit line with a slope of 4.7 μV/mA and R^2 of 0.999. This indicates that a larger AE signal was recorded for increasing current. In the images, the monopole appeared weaker at smaller current, but remained detectable and visible at a current level near 1 mA, consistent with previous phantom experiments [8]. This suggests that the sensitivity using the intracardiac catheter in the cylindrical gel was 4.7 μV/mA and within the range of detecting physiologic current. Effect of recording distance (distance from the recording electrode to the monopole) on UCSDI was also studied (Fig. 3b). Different electrodes on the catheter were used to measure the AE signal, while the current was kept constant. At recording electrodes further away from the monopole, the detected AE signal was smaller in amplitude, but still detectable more than 25 millimeters from the source.

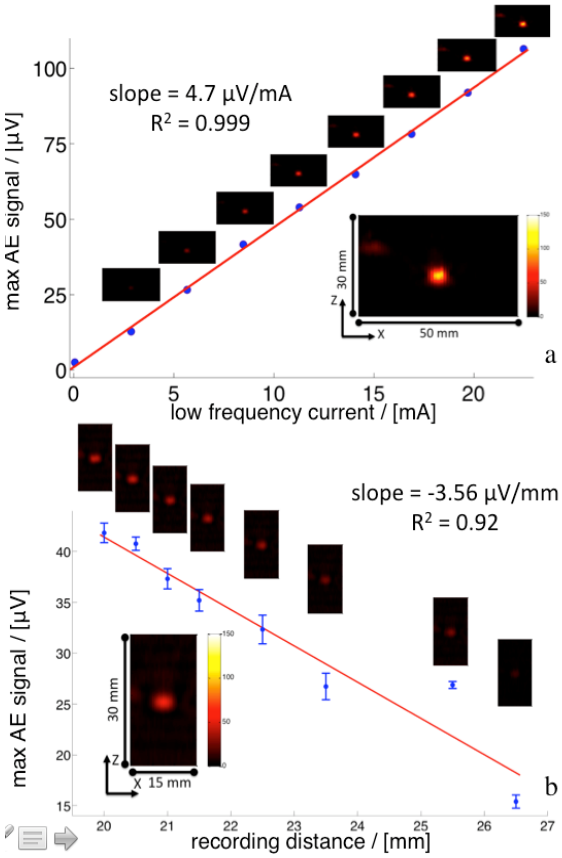

Figure 3. Effect of current amplitude and recording distance on the sensitivity of UCSDI in cylindrical gel. a: AE signal magnitude at various current levels. Red line is the best-fit line with slope of 4.7 μV/mA and R^2 of 0.999. Image of the monopole corresponding to each data point is displayed above the point. The inset is the bigger version of the image corresponding to the highest current level. b: AE signal magnitude at various recording distances. Standard deviation of the multiple measurements for each data point is displayed as an error bar. Red line is the best-fitted line with slope of -3.56 μV/mm and R^2 of 0.92. Image of the monopole corresponding to each data point is displayed above the point. The inset is the bigger version of the image corresponding to the nearest distance. Images are displayed on a linear scale.

B. *Porcine heart*

Fig. 4 depicts results of imaging current injected into the excised porcine heart. A monopole was generated by the electrode pointed by the arrow in Fig. 4b. UCSDI and PE images of the monopole were superimposed to provide more anatomical detail. The position of the monopole relative to the surface of the heart is displayed.

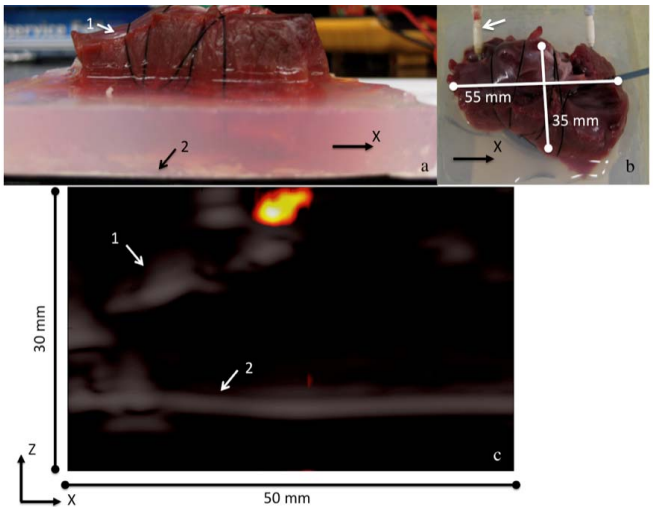

Figure 4. Images of a monopole injected into fresh porcine heart tissue. a: photograph of the excised porcine heart sample. Arrow 1 denotes the curved surface of the heart. Arrow 2 denotes bottom of the gel/heart interface. b: photograph indicating the dimensions of the sample. The arrow points to the electrode that was used to record the AE signals from the interaction between the ultrasound and monopole distribution c: Superimposed UCSDI image (hot) and PE image (gray) of the sample. Arrow 1 points to the location corresponding to the arrow 1 in a. Arrow 2 points to the location corresponding to the arrow 2 in a. Images are displayed in dB scale.

Sensitivity of UCSDI was also investigated in porcine heart tissue using the monopole current pattern. In Fig. 5, AE signal magnitudes measured on the same electrode (recording distance 20 mm) at various current levels are presented. The best-fit line for the data had a slope of 3.2 μV/mA, and a R^2 of 0.92. Smaller AE signals were recorded at smaller currents, consistent with the phantoms experiments and previous publications [8] At a current level of less than 5 mA in porcine heart tissue, the AE signal was readily detectable at recording distance of 20 mm.

IV. Discussion

There is a difference between the sensitivity measured in the gel phantom (4.7 μV/mA, R^2 = 0.999, Fig. 3a) and in porcine heart tissue (3.2 μV/mA, R^2 = 0.92, Fig. 5). This might be due to the heterogeneity of biological tissue. Heterogeneous medium has more variability in the gradient of the current field, which leads to more variability in the measured AE signal

amplitude. The lower sensitivity (slope) in porcine heart tissue than in the cylindrical NaCl gel might be caused by several factors—the difference in the interaction constant *K* of the two materials, differences in conductivity, etc.

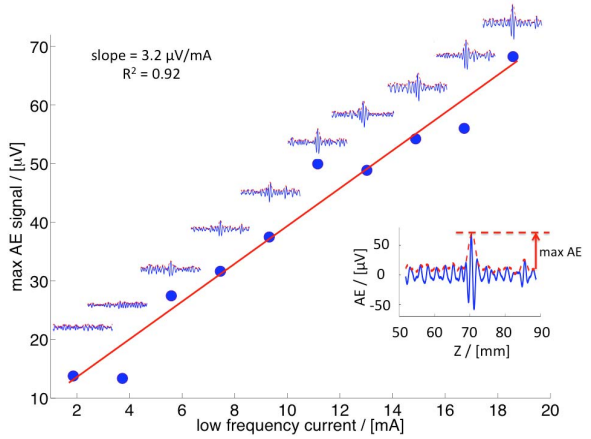

Figure 5. Effect of current amplitude on the sensitivity of UCSDI in porcine heart. Red line is the best-fit line with slope of 3.2 µV/mA and R^2 being 0.92. Envelope and radiofrequency signal corresponding to each data point are displayed above the point. The inset represents the bigger version of the radiofrequency signal corresponding to the highest current level.

CONCLUSION

In this study, we demonstrated UCSDI with a commercial intra-cardiac catheter. Sensitivity of UCSDI with catheter was 4.7 µV/mA (R^2 = 0.999) in cylindrical gel (0.9% NaCl), and 3.2 µV/mA (R^2 = 0.92) in porcine heart tissue. In the future, we will continue to develop UCSDI and interface new technology for translation to the clinic.

REFERENCES

[1] R. M. John and W. G. Stevenson, "Catheter-based Ablation for Ventricular Arrhythmias," *Curr Cardiol Rep*, vol. 13, pp. 399–406, 2011.

[2] D. Bhakta and J. M. Miller, "Principles of Electroanatomic Mapping," *Indian Pacing and Electrophysiology Journal*, vol. 8(1), pp. 32-50, 2008.

[3] V. Markides and D. W. Davies, "New mapping technologies: an overview with a clinical perspective," *Anadolu Kardiyol Derg*, vol. 13, pp. 43–51, 2005.

[4] H. U. Klemm, D. Steven, C. Johansen, R. Ventura, T. Rostock, B. Lutomsky, T. Risius, T. Meinertz, and S. Willems, "Catheter motion during atrial ablation due to the beating heart and respiration: Impact on accuracy and spatial referencing in three-dimensional mapping," *Heart Rhythm*, vol. 4, pp. 587-582, 2007.

[5] F. Duru, "CARTO three-dimensional non-fluoroscopic electroanatomic mapping for catheter ablation of arrhythmias: a useful tool or an expensive toy for the electrophysiologist?" *Anadolu Kardiyol Derg*, vol. 2(4), pp. 330–370, 2002.

[6] R. Olafsson, R. S. Witte, C. Jia, S.-W. Huang, K. Kang, and M. O'Donnell, "Cardiac activation mapping using ultrasound current source density imaging (ucsdi)," *Ultrasonics, Ferroelectrics, and Frequency Control*, 56(3), pp. 565–547, 2009.

[7] R. Olafsson, R. S. Witte, S-W. Huang, and M. O'Donnell, "Ultrasound Current Source Density Imaging," *IEEE Trans. Biomed. Eng*, . 55(7), pp. 1840–1848, 2008.

[8] R. Witte, R. Olafsson, S.-W. Huang, and M. O'Donnell, "Imaging Current Flow in Lobster Nerve Cord Using the Acoustoelectric Effect," *Appl. Phys. Lett.,* vol. 90, 2007.

[9] Q. Li, R. Olafsson, P. Ingram, Z. Wang and R. Witte, "Measuring the Acousto-electric Interaction Constant in Cardiac Tissue Using Ultrasound Current Source Density Imaging," *IEEE Ultrasonics Synposium (IUS) 2011*, pp. 245-248, 2010.

[10] F. E. Fox, K. F. Herzfeld, and G.D. Rock, "The effect of ultrasonic waves on the conductivity of salt solutions," *Physical Review*, vol. 70, pp. 329-339, 1946.

[11] H. Zhang and L. Wang, "Acousto-electric tomography," *Photons Plus Ultrasound: Imaging and Sensing*, *Proc. of the SPIE*, vol. 5320, pp 145-149, 2004.

[12] M. Gendron, R. Guardo and M. Bertrand, "Experimental setup for developing acousto-electric interaction imaging," *Conf Proc IEEE Eng Med Biol Soc,* pp. 2279-2283, 2009.

[13] J. Jossinet, B. Lavandier, and D. Cathignol, "Impedance modulation by pulsed ultrasound," *Ann. NY Acad. Sci.*, vol. 873, pp. 396-407, 1999.

[14] J. Jossinet, B. Lavandier, and D.Cathignol, "The phenomenology of acousto-electric interaction signal in aqueous solutions of electrolytes," *Ultrasonics*, vol. 36, pp. 607-613, 1998.

[15] B. Lavandier, J. Jossinet, and D. Cathignol, "Experimental measurement of the acousto-electric interaction signal in saline solution," *Ultrasonics*, vol. 38, pp. 929-936, 2000.

[16] J. Jossinet, B. Lavandier, and D.Cathignol, "Quantitative assessment of ultrasound-induced resistance change in saline solution," *Ultrasonics*, vol. 38, pp. 150-155, 2000.

[17] Z. Wang, R. Olafsson, P. Ingram, Q. Li, Y. Qin, R. S. Witte, "Four-Dimensional Ultrasound Current Source Density Imaging of a Dipole Field," *Applied Physics Letters*, vol. 99(11), pp. 113701-113703, 2011.